

Electrochemical carbon nanotube field-effect transistor

M. Krüger, M. R. Buitelaar, T. Nussbaumer, and C. Schönberger^{a)}
Institut für Physik, Universität Basel, Klingelbergstr. 82, CH-4056 Basel, Switzerland

L. Forró
Institut de Génie Atomique, École Polytechnique Fédérale de Lausanne, CH-1015 Lausanne, Switzerland

(Received 18 September 2000; accepted for publication 27 December 2000)

We explore the electric-field effect of carbon nanotubes (NTs) in electrolytes. Due to the large gate capacitance, Fermi energy (E_F) shifts of order ± 1 V can be induced, enabling to tune NTs from p to n -type. Consequently, large resistance changes are measured. At zero gate voltage, the NTs are hole-doped in air with $|E_F| \approx 0.3\text{--}0.5$ eV, corresponding to a doping level of $\approx 10^{13}$ cm⁻². Hole-doping increases in the electrolyte. © 2001 American Institute of Physics.
 [DOI: 10.1063/1.1350427]

Carbon nanotubes (NTs), in particular single-wall NTs (SWNTs), are prototype one-dimensional (1D) conductors, which ideally come in two forms, either as metals or semiconductors.¹ This classification assumes, that NTs are undoped. An important parameter is the position of the Fermi energy E_F (the chemical potential) with respect to the charge neutrality point (CNP). For an *undoped* NT E_F coincides with the CNP ($E_F = 0$). Electron (n) or hole (p) doping shifts the Fermi energy up or downwards. If the doping induced Fermi level shifts are larger than the energy separation between the 1D subbands, a semiconducting NT is turned into a metallic one. In previous work on SWNTs the characteristic 1D density-of-states (DOS) was measured,² from which $E_F < 0$ was deduced.³ Hole-doping was also inferred from NT-based field-effect transistors (FETs).¹⁻⁶ In contrast to semiconducting SWNTs, only weak field effects were observed in multiwall NTs (MWNTs).⁵ There are also some early measurements on thin films, which suggest that MWNTs are hole-doped, too.⁷

In this letter, we explore the electrochemically induced field-effect of carbon NTs. The electrochemical gating is so effective that E_F can be determined unambiguously on a single MWNT. An extreme sensitivity of the net doping concentration on the environment, in our case different electrolytes, is observed. Because the doping is reflected in the measured electrical resistance, nanoscaled sensors, such as pH sensors can be envisaged.

Electrochemical gating is studied on single MWNTs with lithographically defined Au contacts evaporated over the NTs [Fig. 1(a)].⁸ The NT-contact structure is fabricated on degenerately doped Si with a 400 nm thick SiO₂ spacer layer. The Si substrate can be used as a gate (“backgate”), see Fig. 1(b). Large changes have been observed in the electrical resistance R of SWNT-based “tube FETs” by using such a back gate (BG). The transconductance can be increased if the gate is placed as close as possible to the NT, ultimately into intimate contact. This is achieved in the present work by immersing the NT into an electrolyte [Fig. 1(c)]. The resistance of the NT devices is measured on a probe stage at room temperature. The stage is complemented

with a micropipette ending in a drawn glass capillary. The pipette is positioned over the device and a small droplet of size ≈ 100 μm is delivered. The droplet size is chosen such that the macroscopically large bonding pads are not immersed in the liquid resulting in negligible leak currents in the resistance measurements. The gate contact is formed by a Pt wire within the glass pipette. If, as sketched in Fig. 1(c), a positive gate voltage U_g is applied, the NT–electrolyte interface is polarized by the attraction of cations. The gate capacitance C_g is formed by the double-layer capacitance which can be very large. Here, we focus on experiments in LiClO₄ electrolytes, used at concentrations of 1–500 mM.

Figure 2 compares the gate effect of a MWNT for two cases: with (a) liquid ion-gate and (b) BG. While the initial electrical resistances R at $U_g = 0$ are comparable, the gate induced changes are very different. dR/dU_g is 2.5 Ω/V in (a) and 570 Ω/V in (b). Hence, liquid–ion gating is by a factor >200 more effective than back gating. Starting from $U_g = 0$, R increases with increasing U_g , which is characteristic for p -type behavior. With BG, this increase persists up to the largest possible gate voltages of ≈ 80 V, where the sample is destroyed. In contrast, $R(U_g)$ has a maximum at $U_g = U_0$ in the electrolyte. The decrease of R for $U_g \geq U_0$ now suggests n -type behavior. The position of the resistance maximum therefore marks the charge–neutrality point of the NT, i.e., $E_F = 0$, if $U_g = U_0 \approx 1$ V. $R(U_g)$ is measured cyclicly. After some cycles, an equilibrium situation is established with a relatively well defined peak position and only weak hysteresis, provided one ramps slowly (10 min per sweep). In this example, R changes by only 20%.

Figure 3 shows another example. It illustrates the time

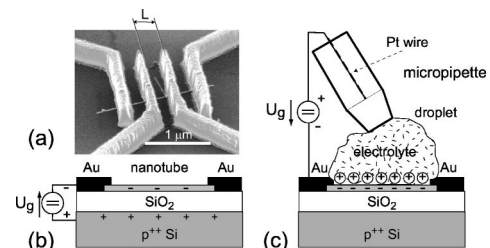


FIG. 1. (a) Typical device consisting of a single MWNT with Au electrodes spaced by $L = 0.3\text{--}2$ μm . The electrical field effect is studied using (b) conventional back gating or (c) liquid–ion gating.

^{a)}Author to whom correspondence should be addressed; electronic mail: christian.schoenberger@unibas.ch

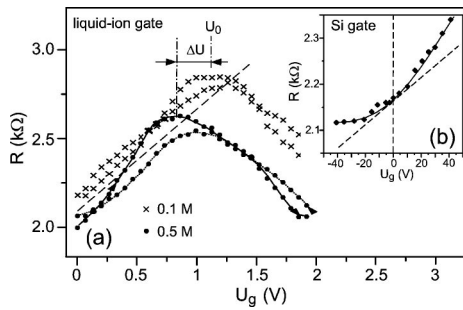


FIG. 2. Electrical resistance R of a MWNT as a function of gate voltage U_g measured (a) in a LiClO_4 electrolyte for two ion concentrations (0.1 and 0.5 M) and (b) in air with BG.

dependence and, most notably, shows a much larger R change. R_{max} is a factor of 5 larger than $R(0)$. Of all our measured samples, approximately half display a weak R change of order 20%–50%, whereas R changes by several 100% for the other half. The first up sweep (increasing U_g) (\times) was followed by a down sweep ($+$). This is repeated until a stationary curve is obtained (\bullet). It is seen that the resistance maximum shifts to higher voltages with time to finally reach $U_0 = 1$ V in this case.

In the following we will present a model which captures the essential physics of this experiment. We assume that only the outermost NT shell needs to be considered⁹ and describe the NT DOS by that of a single layer of graphite, neglecting 1D bandstructure effects.¹⁰ Using the Einstein relation, which relates the diffusion coefficient D to the conductivity, the electrical conductance G can be written as $G = (2\pi r/L)e^2 DN_{\square}$. Here, r is the radius of the NT, L the contact separation, and N_{\square} the two-dimensional (2D) DOS which depends on E_F . For an ideal single sheet of graphite, the DOS is $N_{\square} = 2|E_F|/\pi(\hbar v_F)^2$, where v_F is the Fermi velocity.⁸ At the charge–neutrality point, i.e., at $E_F = 0$, N_{\square} vanishes. We add a phenomenological parameter E_c accounting for a finite DOS at the CNP due to temperature and adsorbate induced band-structure modifications and write $N_{\square} = (2E_c/\pi(\hbar v_F)^2)(1 + (E_F/E_c)^2)^{1/2}$. The normalized conductance $g(E_F) = G(E_F)/G(0) = (1 + (E_F/E_c)^2)^{1/2}$ is used to fit our data. For this $g(U_g)$ is required, so that the relation between U_g and E_F needs to be derived.

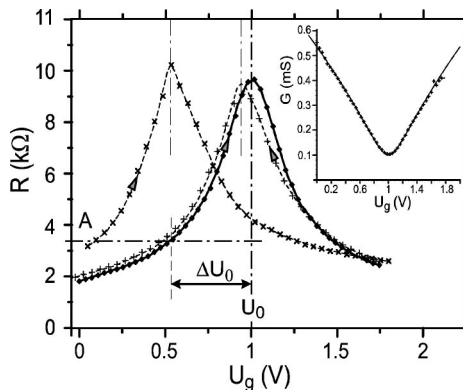


FIG. 3. Electrical resistance $R(U_g)$ of a MWNT measured in a 10 mM LiClO_4 electrolyte. After immersion, the measurement commenced at point A with the data-point sequence \times , $+$, and \bullet (10 min per curve). Drawn curves are guides to the eye. Inset: Comparison of $G = 1/R$ (\bullet) with theory (full curve).

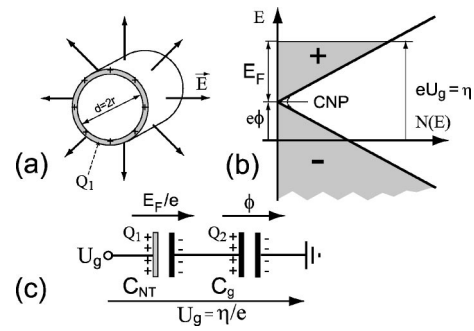


FIG. 4. (a) Single sheet nanotube is assumed to model $R(U_g)$. (b) The energy-dependent DOS under a general biasing condition. CNP denotes the charge-neutrality point, ϕ , E_F , and η the electrostatic, chemical, and electrochemical potentials. (c) A geometrical (C_g) and chemical (C_{NT}) capacitance need to be considered to account for the dependence of $E_F(U_g)$.

Figure 4 shows schematically what happens when a NT is biased via an external gate (engineering sign convention is used here). There are two effects: Firstly, there is an external electric field \vec{E} and correspondingly an electrostatic potential difference ϕ between the NT and the gate electrode. Secondly, E_F must increase because of the addition of charge carriers to the NT. The relations between charges Q_1, Q_2 , [see Fig. 4(c)] and potentials E_F/e , ϕ are determined by the geometrical capacitance $C_g = dQ_2/d\phi$ and chemical capacitance $C_{NT} = dQ_1/d(E_F/e)$ of the NT [Fig. 4(c)]. These two capacitors are in series. Fig. 4(b) shows the energy-dependent DOS for a general biasing condition. The externally applied voltage U_g corresponds to the electrochemical potential η , given by $eU_g = \eta = E_F + e\phi$. From this relation together with $dQ_1 = dQ_2$ and C_g, C_{NT} we obtain

$$e \frac{\partial U_g}{\partial E_F} = 1 + \frac{C_{NT}(E_F)}{C_g}, \quad (1)$$

which provides us with the required relation between U_g and E_F . A significant simplification follows for NTs immersed in electrolytes because $C_g \gg C_{NT}$. This is shown now. The differential NT capacitance per unit length (denoted by C' instead of C) is given by $C'_{NT} = e^2 N'(E_F)$ with $N'(E_F) = 2\pi r N_{\square}(E_F)$. Thus, $C'_{NT} = C'_0(1 + (E_F/E_c)^2)^{1/2}$ with $C'_0 = 4e^2 r E_c / (\hbar v_F)^2$. Taking $r = 5$ nm, $v_F = 10^6$ m/s, and $E_c = 0.1$ eV one obtains $C'_0 \approx 100$ pF/m. The gate capacitance in solution (the double layer capacitance) is $C'_g = 2\pi r \epsilon / \lambda$, where ϵ is the dielectric constant ($\epsilon_{\text{H}_2\text{O}} \approx 80 \times \epsilon_0$), r the NT radius, and λ the screening length $\propto c^{-1/2}$ (c = ion concentration). Taking $c = 0.1$ M, typical numbers are $\lambda \approx 1$ nm and $C'_g \approx 10$ nF/m. If the NT is gated by the Si substrate, a coupling capacitance of $C'_g \approx 5$ pF/m is deduced from our experiments (valid for 300 nm contact separation). Hence,

$$C_g(\text{BG}) \ll C_{NT} \ll C_g(\text{electrolyte}). \quad (2)$$

If the NT is immersed in an electrolyte, the case of interest here, the gate capacitance is much larger than the internal NT capacitance, and we obtain from Eq. (1) a very simple relation $eU_g \approx E_F$, valid for an undoped NT. If it is doped, $Q_2 \neq Q_1$. We denote the doping charge by $Q_d = Q_2 - Q_1$ and the external gate voltage required to induce charge neutrality by U_0 . Since $E_F = 0$ at the CNP, $U_0 = Q_d/C_g$. The effect of doping is simply to shift the functional dependence of E_F versus U_g , so that $E_F \approx e(U_g - U_0)$. The interpretation of

the measured two gate sweeps is now straightforward, because there is a one-to-one correspondence between U_g and E_F . U_0 coincides with the CNP and directly reflects E_F for an unbiased NT (in the engineering convention $E_F > 0$ corresponds to an excess of positive carriers). A substantial hole doping for MWNTs immersed in LiClO_4 is evident, leading to Fermi level shifts of ≈ 1 eV. What is the origin of this considerable hole doping?

Figure 2(a) shows two measurements of the same MWNT for $c = 0.1$ and 0.5 M. If we assume that doping is intrinsic to the NT, for example due to defects or inclusions, the doping charge Q_d should be constant. The relation $U_0 = Q_d/C_g$ predicts that the position of the resistance maxima should shift to lower values with increasing c according to $U_0 \propto c^{-1/2}$. Though a peak shift in the right direction is seen in Fig. 2(a), the magnitude is far too low, suggesting that Q_d is affected by the electrolyte itself. This conclusion is supported by the time dependence shown in Fig. 3. If the NT is immersed into the electrolyte the resistance $R(U_g = 0)$ drops which corresponds to a shift of U_0 to the right. During the first sweep in Fig. 3, $U_0 \approx 0.5$ V, whereas $U_0 \approx 1$ V in all later sweeps. It is clear that $E_F < 0.5$ eV in air before immersion. Hence, we conclude that the electrolyte induces hole doping in the NT, the magnitude of which depends on c . Intercalation of Li-ions can be excluded because this would lead to n -doped NTs. This leaves the perchlorate ion ClO_4^- as the source of doping. This (weakly) oxidizing species seem to adsorb on the NT specifically leading to a charge transfer which partially oxidizes the NT (hole doping). It is evident that this oxidation is weak in the sense that the carbon network of the NT remains intact. If the NT would be eroded, irreversible measurements with a final loss of the conductance would be expected. If ClO_4^- is able to dope NTs by physisorption the same is expected from O_2 in air. A large sensitivity of the NT conductance on different kind of gases, in particular also O_2 , have been reported very recently.¹¹ This scenario is further supported by our measurements in other electrolytes. If a stronger oxidizing electrolyte is used, we observe an additional shift of the $R(U_g)$ curve to the right (additional hole doping). In contrast, the curve shifts to the left in a reducing solvent.

Finally, a quantitative comparison of the experiments with theory is possible. This is demonstrated in the inset of Fig. 3 where a fit (taking the full theory) to the measured conductance G is shown. The fit yields: $E_c \approx 0.12$ eV and $A := C_g/C_0 \approx 10$. The product AE_c only depends on known parameters, like ϵ , v_F , and c , but not on the NT radius r . Our model predicts for this product 0.9 eV which is in good agreement with 1.2 eV obtained from the fit. This agreement proves that the model of a single tube is correct, implying that the electrical current flows preferentially in the outermost shell where most of electrical field is screened. The parameter E_c was introduced to account for a finite DOS at the CNP. $N'(0)$ is found to be $\approx 6 \times$ larger than N'_{1D} of an ideal metallic SWNT, possibly because of dopant induced states.¹² The other class of $R(U_g)$ curves, which show a much weaker resistance change [e.g., Fig. 2(b)] can be fitted too. However, the deduced parameters are inconsistent with

the model of a single tube. In these cases, the current is most likely flowing in inner shells too, explaining the much weaker gate effect.

For the interpretation of previous electrical measurements, the net doping concentration Q_d and the Fermi-level shift for a “virgin” MWNT in air are important. The later can immediately be obtained by comparing R_0 measured in air for $U_g = 0$ with the $R(E_F)$ dependence of the same NT. This is indicated in Fig. 3: the dash-dotted line corresponds to R_0 and ΔU_0 denotes E_F before immersion. Typical values are 0.3–0.5 eV. Comparing this with the average 1D subband spacing $\hbar v_F/2d$ (≈ 33 meV for a 10 nm diameter NT), we conclude that 9–15 subbands may contribute to G instead of 2 for an ideal metallic NT. This finding explains why previous low temperature measurements could be fairly well described by 2D diffusive transport.⁸ A doping-induced $E_F = 0.3$ eV corresponds to a doping concentration of $Q'_d/e \approx 2 \times 10^3 \mu\text{m}^{-1}$, or expressed per surface area to $Q_d/e \approx 0.7 \times 10^{13} \text{cm}^{-2}$ giving approximately one elementary charge per 500 carbon atoms. Finally, estimates for the diffusion constant D can be given, too. We obtain $D = 170 \pm 50 \text{cm}^2/\text{s}$ corresponding to a mean-free path of 35 nm, in agreement with our previous results obtained differently.⁸

MWNTs in air are hole-doped with a (sheet) doping concentration of $\approx 10^{13} \text{cm}^{-2}$ caused by the adsorption of oxygen. If immersed in a LiClO_4 electrolyte doping increases further most likely due to a specific adsorption of the oxidizing species ClO_4^- . Polarizing the NT via an electrolyte allows to move E_F over a wide range, resulting in large resistance changes. NTs are possibly the most sensitive FETs for environmental application, because the mobile NT carriers are in intimate contact with the environment.

This work was supported by the Swiss National Science Foundation. The authors are very grateful to J. Gobrecht for providing the oxidized Si substrates.

¹For a review see C. Dekker, Phys. Today **52**, 22 (1999).

²J. W. G. Wildöer, L. C. Venema, A. G. Rinzier, R. E. Smalley, and C. Dekker, Nature (London) **391**, 59 (1998); T. W. Odom, J.-L. Huang, P. Kim, and C. Leiber, *ibid.*

³L. C. Venema, J. W. Janssen, M. R. Buitelaar, J. W. G. Wildöer, S. G. Lemay, L. P. Kouwenhoven, and C. Dekker, Phys. Rev. B **62**, 5238 (2000); Y. Xue and S. Datta, Phys. Rev. Lett. **83**, 4844 (1999).

⁴S. J. Tans, A. R. M. Verschueren, and C. Dekker, Nature (London) **393**, 49 (1998).

⁵R. Martel, T. Schmidt, H. R. Shea, T. Hertel, and Ph. Avouris, Appl. Phys. Lett. **73**, 2447 (1998).

⁶C. Zhou, J. Kong, and H. Dai, Appl. Phys. Lett. **76**, 1597 (2000).

⁷S. N. Song, X. K. Wang, R. P. H. Chang, and J. B. Ketterson, Phys. Rev. Lett. **72**, 697 (1994); G. Baumgartner, M. Carrard, L. Zuppiroli, W. Basca, W. A. de Heer, and L. Forró, Phys. Rev. B **55**, 6704 (1997).

⁸C. Schönenberger, A. Bachtold, C. Strunk, J.-P. Salvetat, and L. Forró, Appl. Phys. A: Mater. Sci. Process. **69**, 283 (1999).

⁹A. Bachtold, C. Strunk, J.-P. Salvetat, J.-M. Bonard, L. Forró, T. Nussbaumer, and C. Schönenberger, Nature (London) **397**, 673 (1999).

¹⁰This is justified, because $k_B T$ is of order of the subband separation at room temperature and because of the relatively short electron-mean free path $l \lesssim 2\pi r$ measured in MWNTs.

¹¹J. Kong, N. R. Franklin, C. Zhou, M. G. Chapline, S. Peng, K. Cho, and H. Dai, Science **287**, 622 (2000); P. G. Collins, K. Bradley, M. Ishigami, and A. Zettl, Science **287**, 1801 (2000).

¹²S.-H. Jhi, S. G. Louie, and M. Cohen, Phys. Rev. Lett. **85**, 1710 (2000).